Computational Materials Science 151 (2018) 196–203

Contents lists available at ScienceDirect

Computational Materials Science

journal homepage: www.elsevier.com/locate/commatsci

Effect of sample size, temperature and strain velocity on mechanical properties of plumbene by tensile loading along longitudinal direction: A molecular dynamics study

Dhiman Kumar Das[a,*], Jit Sarkar[b], S.K. Singh[a]

[a] Department of Mechanical Engineering, Indian Institute of Technology (Indian School of Mines), Dhanbad 826004, Jharkhand, India
[b] Department of Metallurgical and Materials Engineering, Indian Institute of Technology, Kharagpur 721302, West Bengal, India

ARTICLE INFO

Keywords:
Plumbene
Two-dimensional nanomaterials
Molecular dynamics
Mechanical properties

ABSTRACT

In recent years, two-dimensional (2D) nanomaterials have received tremendous attention due to their unique structure and extraordinary properties. Graphene, silicene, germanene and stanene- the 2D allotropes of carbon, silicon, germanium and tin have been reported in last few years and their properties have been studied elaborately. Plumbene, the 2D allotrope of lead, is recently reported. It is analogous to graphene, silicene, germanene and stanene in single-layered and hexagonal arrangement of atomic structure. In this paper, molecular dynamics simulations have been carried out to study the effect of sample size, temperature and strain velocity on the mechanical properties of plumbene. The results show superior mechanical properties of the single layer plumbene sheet which is several times higher than bulk lead making it a suitable candidate for using as reinforcement to develop high strength nanocomposites.

1. Introduction

Reduction in dimensionality of a material reduces the available phase space and diminishes screening which lead to enriched quantum effects and increased corrections. As a result these materials exhibit exceptional properties. Nanomaterials have wide range of potential applications due to enhanced mechanical, electrical, thermal, optical and chemical properties than bulk materials. [1–7] Graphene, the two-dimensional allotrope of carbon, due to its impressive mechanical and thermal [6–8] properties is widely used now-a-days in industries [9,10] where mechanical stability and thermal conductivity are the main concerns. Silicene, germanene and stanene also have promising properties for wide range of applications [11–13].

Plumbene [14–16] is a single layer of sp-hybridized lead atoms tightly packed into a two-dimensional hexagonal structure analogous to graphene and other members of the group. Pb-Pb bond distance in plumbene is 3 Å. This 2D nanomaterial has a large band gap of ~400 meV which is higher than other topological materials with band gap of ~200 meV [15]. Graphene have no band gap normally but a band gap of 2 meV can be induced in it by doping silicene as n-type dopant in graphene [17]. Silicene itself have a band gap of ~20 meV approx. Hence band gap of plumbene is even greater than graphene and silicene [18]. Like plumbene silicene is also more stable in buckled structure than planar structure and have the tendency to form sp^2 hybridization [19]. Silicon possesses higher band gap 1.25 to > 3 eV under different operational conditions than plumbene [20,21]. Germanene have interatomic distance and band gap of 4.061 Å and 0.06 eV [22,23]. By proximity coupling of graphene to antiferromagnetic material quantum anomalous Hall effect is realized in it and it also have stronger hybridization than plumbene (topological insulator) [24]. Quantum Anomalous Hall (QAH) effect is also observed in other hexagonal metal-oxide Nb_2O_3 which results its application as a topological insulator [25]. Similarly stanene, the honeycomb-like structures of tin atoms have strongest spin-orbit-coupling (SOC) effect for which the nontrivial topological insulator state can drive and stabilized by them. This also gives rise to new Quantum Spin Hall effect (QSH) insulators in stanene film [26,27]. QSH phenomenon is also noticed in functionalized Bi/Sb(1 1 1) films and thus they found application as a dissipationless transport device at room temperature [28]. But nanomaterials have many other advantages over bulk materials hence targeted to be used replacing conventional bulk materials. Zhao et al., also have predicted very high band gap of 1.03 eV to 1.34 eV in plumbene by

* Corresponding author.
E-mail address: gournetaidas@rocketmail.com (D.K. Das).

https://doi.org/10.1016/j.commatsci.2018.05.006
Received 31 December 2017; Received in revised form 10 April 2018; Accepted 4 May 2018

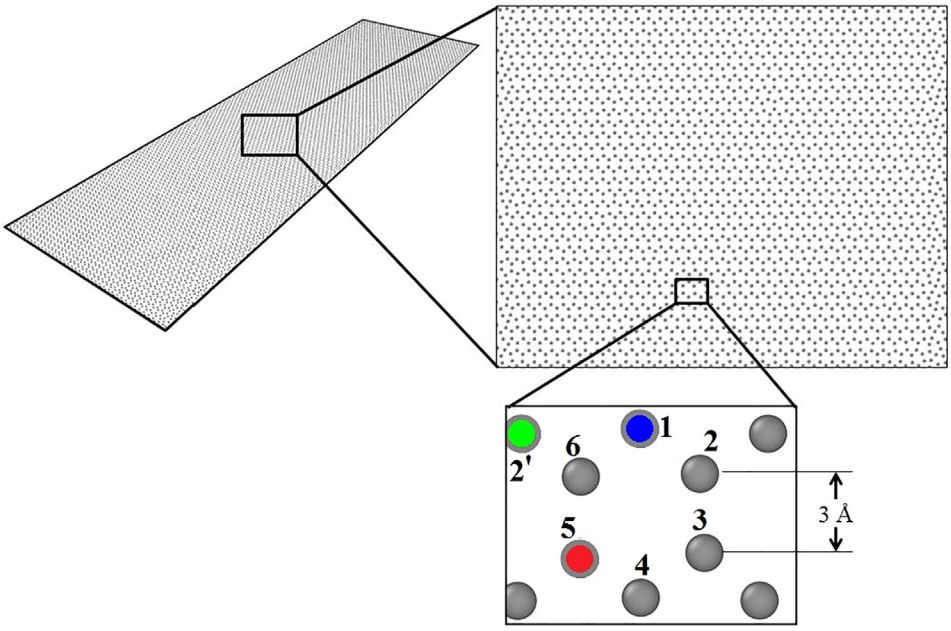

Fig. 1a. Our designed plumbene sheet (planar structure).

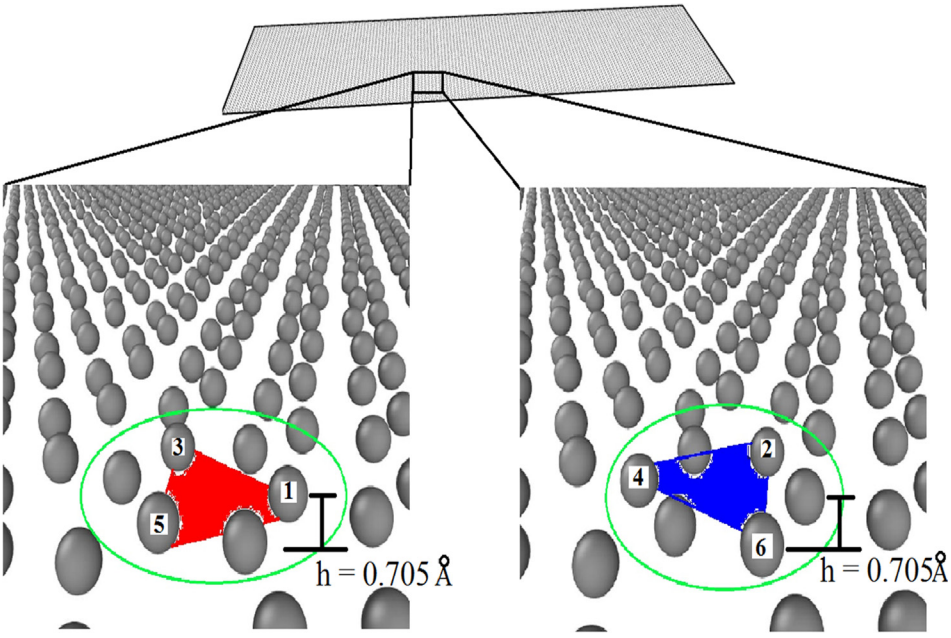

Fig. 1b. Our designed plumbene sheet (buckled structure).

doping different types of halides in it [16]. The buckling structure of plumbene enhances the overlap between σ and π orbitals. With increase in molecular weight of materials the type of hybridization changes from sp^2 to sp^3[14]. Plumbene is still a predicted material whose few properties like band gap, mechanism of hybridization among its bonds, structural symmetry are being calculated using first principal calculations and computational modeling. Experimental synthesis of plumbene is not reported till now. We have estimated the mechanical properties of plumbene using molecular dynamics simulations under tensile loading. The variation of mechanical properties of plumbene with variation in sample size, temperature, strain velocity and axis of loading are also reported here. The novelty of our work is earlier no such work of estimating mechanical properties of plumbene is reported. We found our estimated values of mechanical properties of plumbene like Young's modulus (E) and ultimate tensile strength (UTS) are much higher than bulk lead with E and UTS values 16 GPa and 12 to 17 MPa. Due to this band gap plumbene can found its applications as topological insulators and high temperature applications [15,16]. Plumbene with high

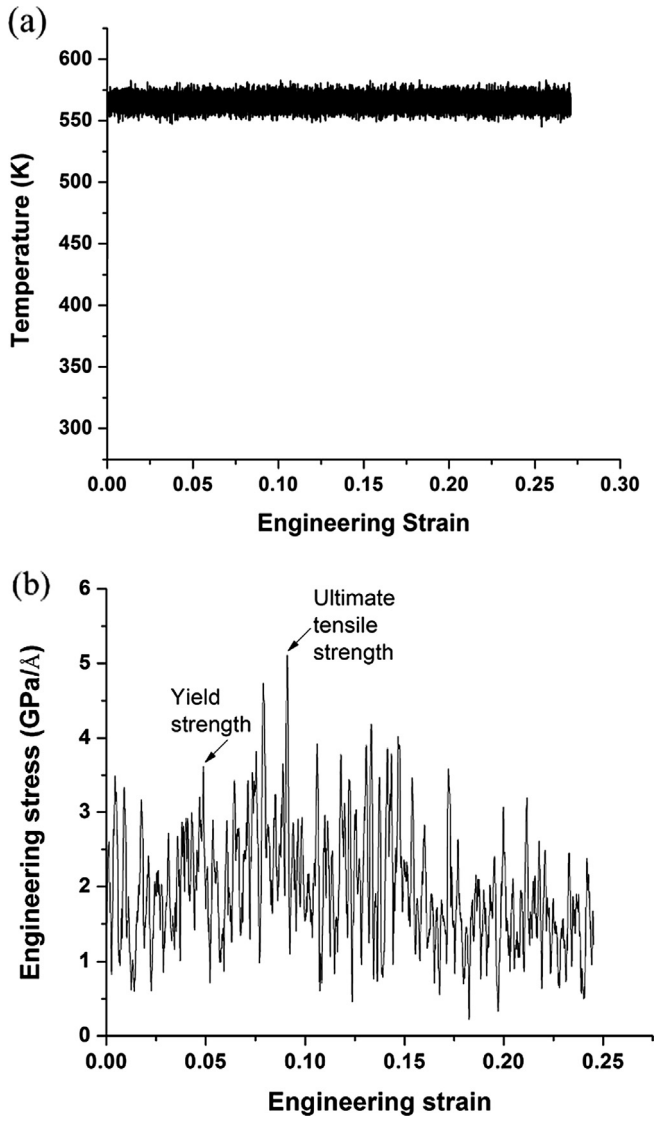

Fig. 2. Plot of (a) temperature vs strain and (b) engineering stress vs engineering strain of a plumbene sheet.

mechanical stability can be utilized as materials where mechanical strength is the prime concern. It can be reinforced in bulk materials to enhance its mechanical properties forming new nanocomposites.

Functions and physical basis of atomic and molecular structures are very well understood by molecular dynamics (MD) simulation method. Ultimate details about individual atoms can be provided by MD simulation which concern motion of particles as a function of time. Properties of a system are often addressed more easily by MD simulations than actual experiments which are sometimes difficult to perform due to experimental limitations. The potential used in MD simulations are completely user defined thus giving us the choice to define the role of this process in evaluating desired properties of a model system [31].

In our work, we have used MD simulation technique to predict the mechanical properties of plumbene under varying parameters. Literature survey shows that mechanical properties of plumbene are not yet being investigated so far. In this paper, we have investigated the mechanical properties like yield strength (YS), ultimate tensile strength (UTS) and Young's modulus (E) of armchair plumbene sheet with variation in sample size, temperature and strain rate using MD simulation method.

2. Simulation procedure

To perform simulation for evaluating mechanical properties of plumbene we have used LAMMPS [33] (Large-scale Atomic/Molecular Massively Parallel Simulator) Molecular Dynamics Simulator. Using inbuilt crystal structure generation algorithm [29] in LAMMPS we have designed a 700 × 200 Å^2 plumbene sheet. Velocity-Verlet algorithm is used here to determine the interacting nature between atoms. Fig. 1a shows our initially generated plumbene sheet having armchair direction orientation of its atoms with length 700 Å in the y-direction and width of 200 Å in the x-direction respectively. The visualization software OVITIO [30] is used to observe the incidents occurring during simulation of the sheet.

Fig. 1b shows side view of buckled structure plumbene sheet. Both the macroscopic view of the same section of buckled plumbene sheet is shown here. In the right hand section shows atoms 2, 4 and 6 are in one plane (blue[1] plane) little below from the left hand section atoms 1, 3 and 5 which are in another plane (red plane). The difference between these two planes of atoms is the buckling height of plumbene whose value is found 0.705 Å.

For equilibration of plumbene sheet at 298 K temperature, MD simulation is performed with progressing time steps of 1 fs to determine the phases of atoms in the sheet. The accuracy of the MD simulations and the results obtained from it depends on the choice of accurate interatomic potential function. The many body dependence of the potentials is efficiently incorporated in an embedding energy system along with a pairwise energy term by embedded atom method (EAM) potential known as EAM potential [31,32] which was developed by Daw and Baskes. Hence, for close-packed transition metals the properties like lattice and elastic constants, cohesive energies, and the vacancy formation energies are well described by EAM potentials. The total energy of the atoms using EAM potential is given by:

$$E = \frac{1}{2}\sum_{i,j,i\neq j}\phi_{ij}(r_{ij}) + \sum_{i} F_i(\rho_i) \tag{1}$$

where ϕ_{ij} is the pair energy between atom i and j separated by distance r_{ij} and F_i is the embedding energy associated with embedding an atom i into a local site with an electron density ρ_i. The electron density is given by:

$$\rho_i = \sum_{j,j\neq i} f_j(r_{ij}) \tag{2}$$

where $f_j(r_{ij})$ is the electron density of atom i at a distance r_{ij} from atom j. For our plumbene sheet EAM/alloy potential is used. The elemental pair potential is given by

$$\phi(r) = \frac{A\exp[-\alpha(r/r_e-1)]}{1+|(r/r_e-k)|^{20}} - \frac{B\exp[-\beta(r/r_e-1)]}{1+|(r/r_e-\lambda)|^{20}} \tag{3}$$

where the distance between two nearest atom is r_e, k and λ are the parameters for cutoff radius and A, B, α and β are the four adjustable parameters [31,32]. Spin-orbit coupling effect is one important phenomenon among electrons of lead [33]. EAM/alloy potential accounts this property and thus ensures accuracy for estimating mechanical properties of plumbene [34,35].

Nose-Hoover thermostat [36] is used to maintain a constant temperature during both equilibrations. In our MD simulation, the force calculation is based on Newton's second law of motion:

$$m_i\frac{d^2x_i(t)}{dt^2} = f_i \equiv -\frac{\partial U}{\partial x_i}, \tag{4}$$

where in the x-direction m_i, f_i and $\frac{d^2x_i(t)}{dt^2}$ are the mass, force and acceleration on i_{th} atom respectively and ∂U is the energy of i_{th} atom.

[1] For interpretation of color in Fig. 1b, the reader is referred to the web version of this article.

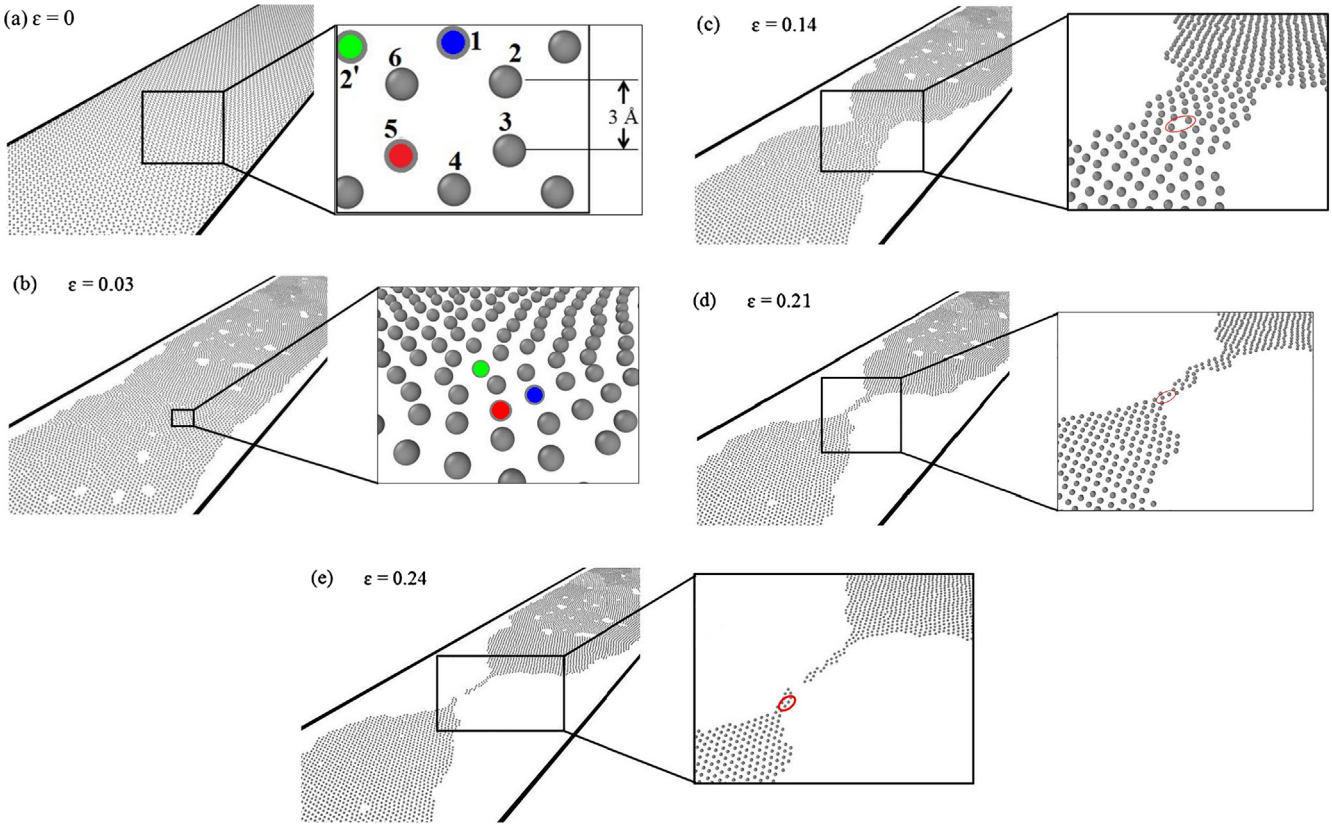

Fig. 3. Plumbene sheet (a) after equilibration, (b) initiation of tensile loading, (c) necking during tensile loading, (d) just before rupture and (e) final failure.

Velocity-Verlet algorithm is used to obtain the position and velocity of atoms of plumbene sheet at a particular instant of time *t*. For increment in time Δt the positions and velocities of each atom are updated from the previous step at every instant of time. The equations used for this purpose are:

$$x_i(t_0 + \Delta t) = x_i(t_0) + v_i(t_0)\Delta t + \frac{1}{2}\left(\frac{f_i(t_0)}{m_i}\right)(\Delta t)^2, \tag{5}$$

$$v_i(t_0 + \Delta t) = v_i(t_0) + \frac{1}{2}\left[\frac{f_i(t_0)}{m_i} + \frac{f_i(t_0 + \Delta t)}{m_i}\right]\Delta t, \tag{6}$$

where $x_i(t_0)$, $v_i(t_0)$ and $\frac{f_i(t_0)}{m_i}$ are the position, velocity and acceleration of i_{th} atom in x-direction at time instant t_0; and $x_i(t_0 + \Delta t)$, $v_i(t_0 + \Delta t)$ and $\frac{f_i(t_0+\Delta t)}{m_i}$ are the position, velocity and acceleration of i_{th} atom in x-direction at time instant $(t_0 + \Delta t)$ [37].

The designed sample is equilibrated at room temperature (298 K) for 20 ps with a time step of 1 fs. After equilibration, the tensile testing of the sample is carried out in analogous to real tensile testing experiment and the sample was loaded in y-direction. One-sixth of the total length of the sample is kept fixed at one end and another one-sixth portion of the sample at the other end is displaced along the y-direction i.e. longitudinal direction, at a constant strain velocity of 1 Å/ps. It is found that there are 11,573 atoms in our designed plumbene sheet of dimension 200 × 1100 Å^2. We have calculated the yield strength, ultimate tensile strength and Young's modulus. To study the effect of sample size on mechanical properties, plumbene sheet having fixed width of 200 Å and varying length from 700 to 1500 Å have been studied. A variation in sizes from 700, 900, 1100, 1300 and 1500 Å in length is done and mechanical properties are evaluated for all the samples. These sample sizes are chosen for 2D materials for real experimental tests. They are the representative volume elements (RVEs) for plumbene sheets with other dimensions and are predicted to have same materialistic properties. The effect of temperature on mechanical properties has been studied on a plumbene sheet of dimension 200 × 1100 Å^2 by varying the temperature from 318 to 398 K. To study the effect of strain velocity on mechanical properties, plumbene sheet having dimension 200 × 1100 Å^2 have been studied for strain velocity of 0.1 to 6 Å/ps.

3. Results and discussions

Young's modulus (E) is the proportionality constant of longitudinal (tensile or compressive) stress to longitudinal strain of a bar sample of any geometry within elastic limit. The capacity of a material to withstand with maximum load against tensile deformation is its ultimate tensile strength (UTS). Yield strength of a material is the stress at which it begins to deform plastically [38]. The variation of temperature and engineering stress with engineering strain is shown in Fig. 2(a) and (b) respectively. It is observed that the temperature increases and the entire deformation process occurs at a constant temperature of 565 K with some fluctuations. Thermostating was done during equilibration of plumbene sheet to room temperature before deformation. No thermostating was done during the tensile loading and thus results in increase in temperature of the sheet during tensile loading, as a consequence of the plastic deformation occurring in the sheet. The plots of engineering stress vs. strain shows that the stress increases almost linearly till elastic limit or yield point (yield strength marked in Fig. 2(a)) up to a strain of ε = 0.05, following Hooke's law. Then there is a sharp drop in stress with the initiation of dislocations movement and plastic flow begins.

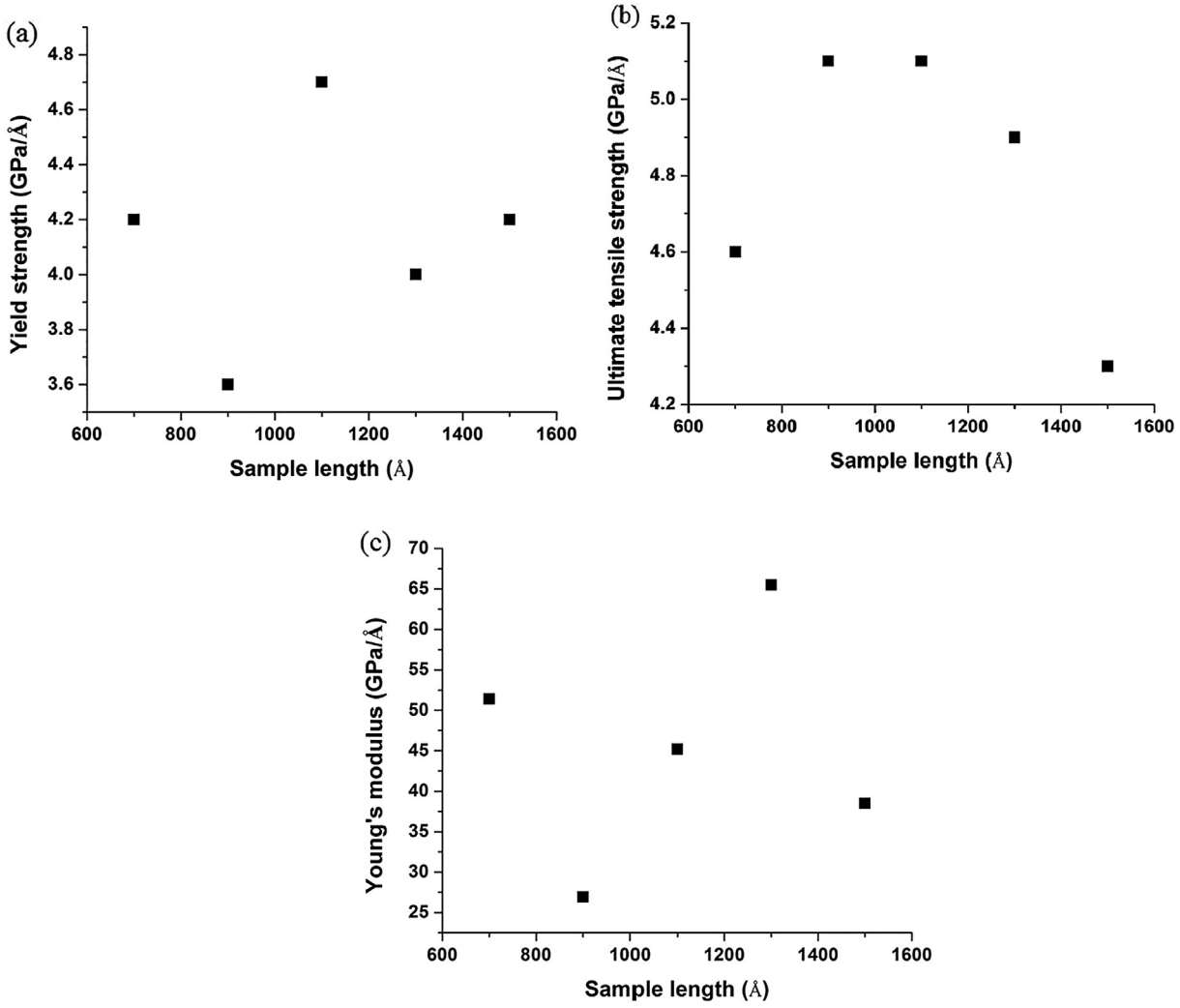

Fig. 4. Variation of (a) yield strength, (b) ultimate tensile strength and (c) Young's modulus of plumbene sheet with sample length.

The stress gradually increases again due to obstruction in dislocations movement and finally reaches the maximum stress or ultimate tensile strength (UTS) (as shown in Fig. 2(a)) at a strain of $\varepsilon = 0.09$. After UTS, the dislocations overcome the barrier and move freely. The stress gradually decreases followed by initiation of necking and the sample finally fail in a ductile manner at the final strain of $\varepsilon = 0.24$. The overall curve has some fluctuations due to atomic vibrations as the simulations are done in nanoscale. Fig. 3 shows sequence wise events of tensile deformation of plumbene sheet having dimension 200×1100 Å^2.

The yield strength, ultimate tensile strength and Young's modulus for different samples are obtained from the respective engineering stress vs. strain curves and their variation with sample length (with constant sample width of 200 Å) is shown in Fig. 4.

It is observed from Fig. 4(a) that the yield strength of plumbene sheet decreases sharply from sample length of 700 to 900 Å after which it linearly increases up to 1500 Å along with a sharp rise at 1100 Å. The sharp rise in yield strength at 1100 Å can be attributed to the very good elasticity of plumbene at that critical sheet size, after which it decreases and again increase in a linear manner to lower yield strength values. From Fig. 4(b) it is observed that the ultimate tensile strength of plumbene sheet increases sharply from sample length of 700 to 900 Å, then remains constant from 900 to 1100 Å, after which it decreases gradually from 1100 to 1500 Å with a sharp drop from 1300 to 1500 Å. The sheet length of 900 Å shows good plastic deformation behaviour with very high strength similar to that shown by the critical sheet size of 1100 Å. It is observed from Fig. 4(c) that the Young's modulus of plumbene sheet decreases sharply from sample length of 700 to 900 Å, then linearly increases from 900 to 1300 Å followed by a sharp decrease again from 1300 to 1500 Å. The sheet size of 900 Å shows the least resistance to elastic deformation. The sheet size of 1100 Å shows more resistance to elastic deformation than the sheet size of 900 Å. So the critical sheet size of 1100 Å shows the best mechanical property.

The variation of yield strength, ultimate tensile strength and Young's modulus with temperature is shown in Fig. 5.

It is observed from Fig. 5(a) that the yield strength of plumbene sheet gradually increases from 318 to 358 K with a sharp rise from 338 to 358 K and it gradually decreases from 358 to 398 K with a sharp drop from 378 to 398 K. The sheet size of 1100 Å shows the highest yield strength at a temperature of 358 K but it is lower than the yield strength observed at room temperature. This can be attributed to the increase in vibration of the atoms with rise in temperature. From Fig. 5(b) it is observed that the ultimate tensile strength of plumbene sheet decreases

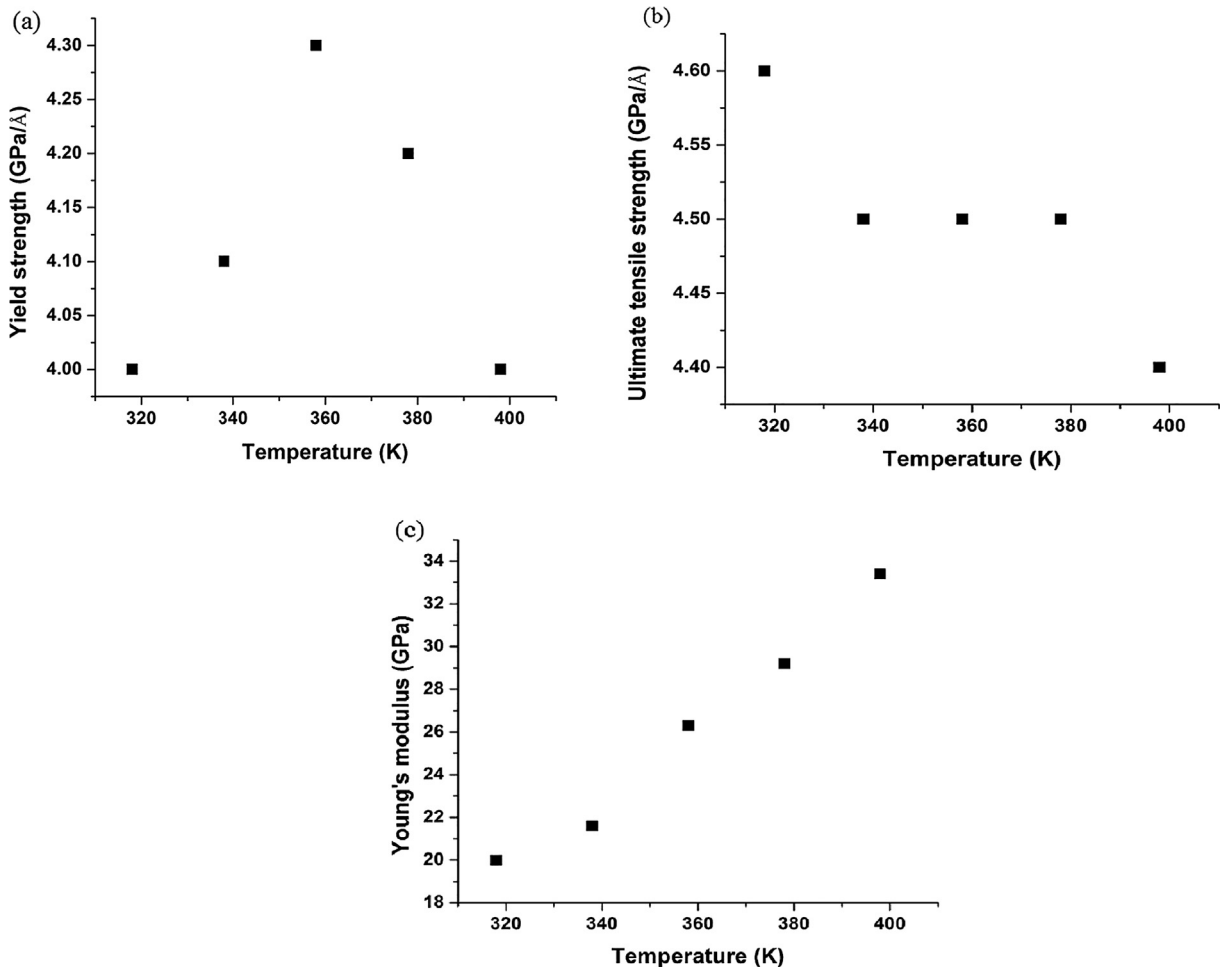

Fig. 5. Variation of (a) yield strength, (b) ultimate tensile strength and (c) Young's modulus of plumbene sheet with temperature.

from 318 to 338 K after which it remains constant from 338 to 378 K and then it decreases from 378 to 398 K. The ultimate tensile strength of the sheet is not affected by temperature over a range of 338 to 378 K thus maintaining its good plastic deformation behaviour which again decreases with further rise in temperature. But the values have decreased than that observed at room temperature due to the increase in atomic vibrations with rise of temperature. It is observed from Fig. 5(c) that the Young's modulus of plumbene sheet gradually increases from 318 to 398 K with a sharp rise from 338 to 358 K and from 378 to 398 K. The rise in temperature increases the atomic vibrations of the sheet and thus the sheet shows more resistance to elastic deformation with rise of temperture.

The variation of yield strength, ultimate tensile strength and Young's modulus with strain velocity is shown in Fig. 6.

It is observed from Fig. 6(a) that the yield strength of plumbene sheet increases sharply from strain velocity of 0.1 to 1 Å/ps after which it slightly decreases from 1 to 2 Å/ps and then it remains constant up to strain velocity of 6 Å/ps. The sheet size of 1100 Å shows highest elastic deformation behaviour at a strain velocity of 2 Å/ps after which it decreases as deformation is occurring at a faster rate causing the atoms to rupture quickly. Then the elastic deformation behaviour of the sheet shows no change with faster loading rate. From Fig. 6(b) it is observed that the ultimate tensile strength of the plumbene sheet increases sharply from strain velocity of 0.1 to 1 Å/ps after which it slightly increases from 1 to 2 Å/ps. The sheet shows good plastic deformation behaviour with the maximum at the strain velocity of 2 Å/ps after which the atoms rupture at a very faster rate with further increase in strain velocity. Strain velocity above 2 Å/ps shows that the deformation occurs mostly in an elastic manner and no ultimate tensile strength is observed. The plumbene sheet reaches its yield strength after which failure occurs in a brittle manner. This can be attributed to the faster rupturing of the atoms with the increase in loading rate. Thus a ductile to brittle transition in the mode of fracture is observed above a strain velocity of 2 Å/ps. It is observed from Fig. 6(c) that the Young's modulus of plumbene sheet slightly increases from strain velocity of 0.1 to 1 Å/ps followed by a sharp increase from 1 to 2 Å/ps after which it slightly increases from 2 to 4 Å/ps and then it decreases sharply from 4 to 6 Å/ps. The resistance of the sheet to elastic deformation gradually increases with increase in strain velocity showing maximum resistance at a strain velocity of 4 Å/ps. It then decreases due to increase in loading rate which causes the atoms to rupture quickly. Fig. 7 shows the sequence of deformation behaviour of plumbene sheet in a brittle manner above a strain velocity of 2 Å/ps.

3-fold coordination in observed in single layer plumbene with hexagonally arranged six atoms in each unit cell (Fig. 1). The magnified images showing coordination of a single atom of our plumbene sheet

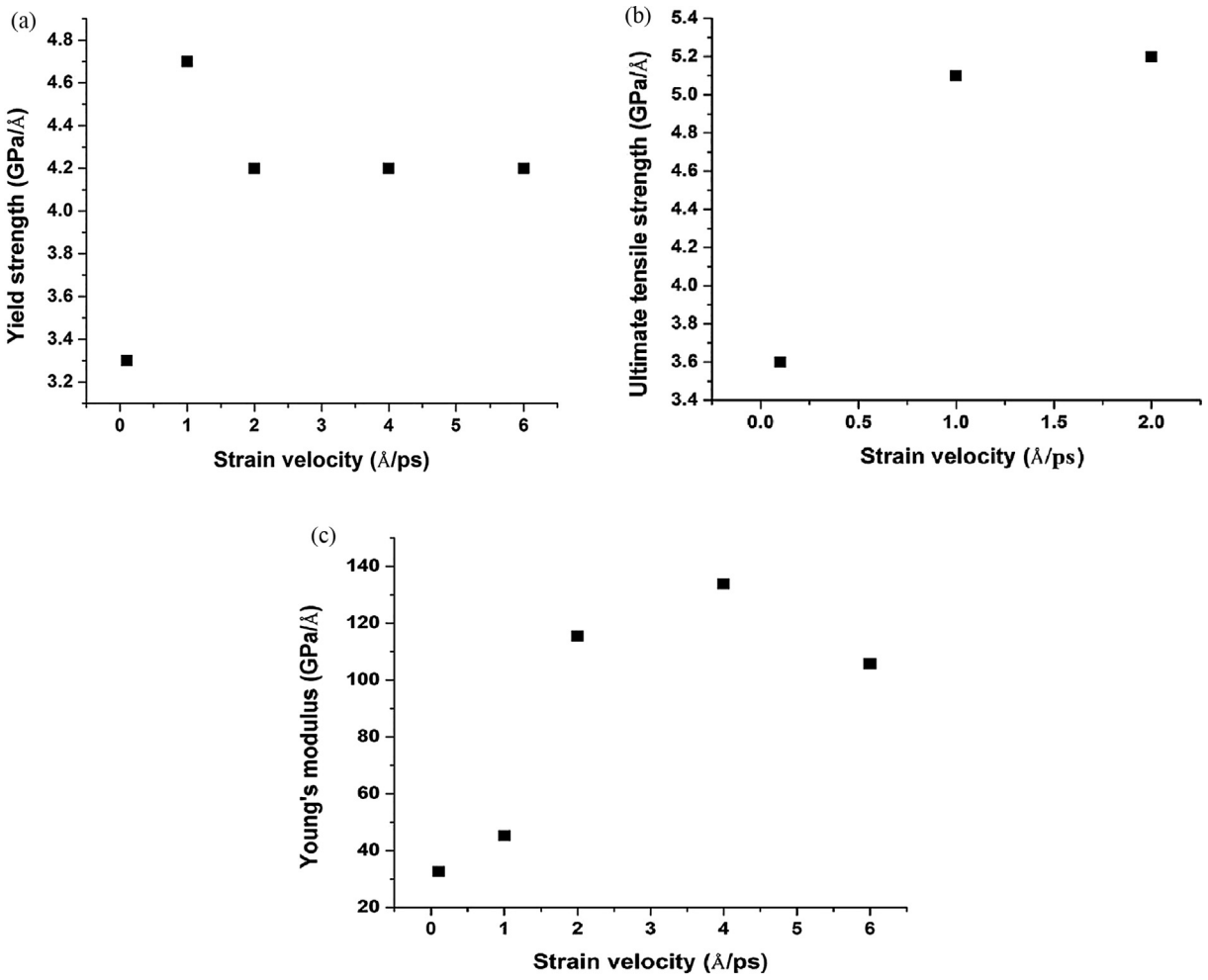

Fig. 6. Variation of (a) yield strength, (b) ultimate tensile strength and (c) Young's modulus of plumbene sheet with strain velocity.

just after equilibration, during tensile loading condition and of the edges during rupture of the sheet (both tensile loading and equilibrium MD) in Figs. 3(b)–(e), 7(b) and (c) respectively. The interatomic distances between each atom of a plumbene sheet leading to 2-fold coordination during loading and rupture of the sheet are also shown.

From above graphs we observe the mechanical properties i.e. ultimate tensile strength and Young's modulus of plumbene sheets with different configurations under different temperatures and strain velocity are higher than bulk lead. Hence, plumbene claims superior mechanical properties than bulk lead with ultimate tensile strength and Young's modulus of 12–17 MPa and 16 GPa respectively. However, the theoretically calculated ultra-high mechanical properties of plumbene may differ from real experimental values due to the factors like our modelled sample is a perfect uniform crystal structure in the absence of internal defects and the simulations have been carried out under ultra-high strain velocities due to computational limitations in nanoscale.

4. Conclusion

In this paper, the mechanical properties like yield strength, ultimate tensile strength and Young's modulus of single-layered 2D plumbene sheets and the effect of sample size, temperature and strain velocities on these mechanical properties was studied using molecular dynamics simulations. The study of the effect of sample size variation shows that the plumbene sheet of dimension 200×1100 Å^2 shows highest yield strength among the investigated samples, highest ultimate tensile strength among the investigated samples is exhibited by both the samples of dimension 200×900 Å^2 and 200×1100 Å^2. On the other hand, the sample of dimension 200×1300 Å^2 shows highest Young's modulus among the investigated samples. The study of the effect of temperature variation on the plumbene sheet of dimension 200×1100 Å^2 shows highest yield strength at a temperature of 358 K, highest ultimate tensile strength at a temperature of 318 K and highest Young's modulus at a temperature of 398 K. The Young's modulus continuously increases with increasing temperature of the plumbene sheet. The study of the effect of strain velocity on the plumbene sheet of dimension 200×1100 Å^2 shows highest yield strength at a strain velocity of 1 Å/ps, highest ultimate tensile strength at a strain velocity of 2 Å/ps and highest Young's modulus at a strain velocity of 4 Å/ps. The study also shows that there is a transition from ductile to brittle in the mode of fracture above a strain velocity of 2 Å/ps. The mechanical properties of plumbene obtained under varying conditions are several times greater than that of bulk lead. The results favour use of such an attractive material as reinforcing agent to develop different nanocomposites with high strength and excellent material properties.

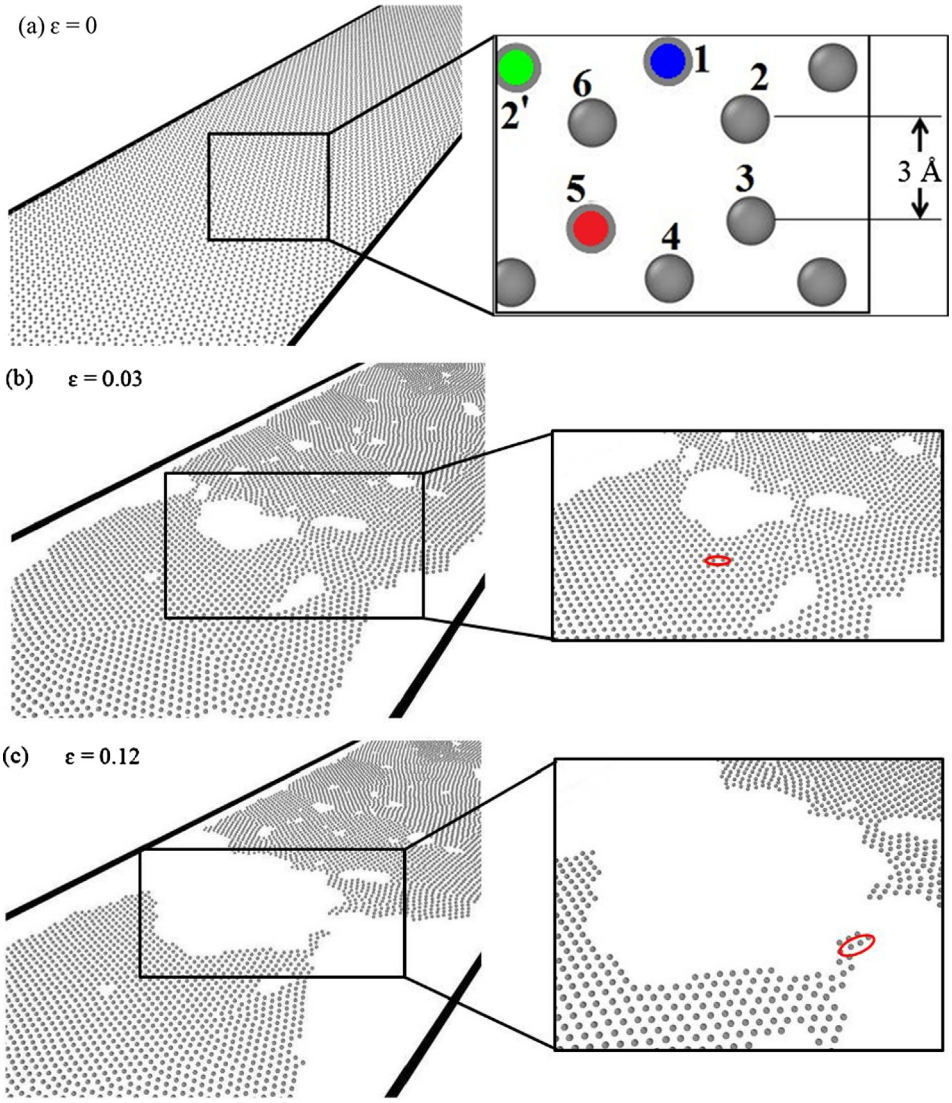

Fig. 7. Brittle fracture of plumbene sheet above strain velocity of 2 Å/ps.

Conflict of interest

The authors declare that there is no conflict of interest in the present work.

References

[1] K. Arivalagan, et al., Int. J. Chem Tech Res. 3 (2) (2011) 534.
[2] S.K. Bhullar, et al., Rev. Adv. Mater. Sci. 44 (2016) 286.
[3] H. Fuchs, et al., ChemPhysChem 13 (2012) 2423.
[4] F. Iskandar, Adv. Powder Technol. 20 (2009) 283.
[5] D. Guo, et al., J. Phys. D Appl. Phys. 47 (2014) 013001.
[6] Q. Li, Nanomaterials for Sustainable Energy, Springer Publishing, 2017.
[7] A.K. Geim, K.S. Novoslov, Nat. Mater. 6 (2007) 183.
[8] K.S. Novoselov, et al., Nature 490 (2012) 192.
[9] X. Wang, et al., Nano Lett. 8 (2008) 323–327.
[10] J.S. Moon, et al., IEEE Electron Device Lett. 30 (6) (2009) 650.
[11] S. Kaneko, et al., Appl. Phys. Express 7 (2014) 035102.
[12] L. Matthes, et al., J. Phys..: Condens. Matter 25 (2013) 395305.
[13] M.J.S. Spencer, T. Morishita, Silicene: Structure, Properties and Applications, Springer Publishing, 2016.
[14] P. Rivero, et al., Phys. Rev. B 90 (2014) 241408.
[15] X. Yu, et al., Phys. Rev. B 95 (2017) 125113.
[16] H. Zhao, et al., Sci. Rep. 6 (2016) 20152.
[17] D.K. Das, S. Sahoo, Intelligent Computing and Applications, Graphene–Silicene Composite can Increase the Efficiency of Cloud Computing, Springer Publishing, 2015.
[18] N.D. Drummond, et al., Phy. Rev. B 85 (2012) 075423.
[19] C. Zhang, S. Yan, J. Phys. Chem. C 116 (2012) 4163–4166.
[20] J.J. Low, et al., Am. J. Undergraduate Res. 7 (1) (2008) 27–32.
[21] C. Harris, E.P. O'Reilly, Physica E 32 (2006) 341–345.
[22] S.C. Wu, et al., PRL 113 (2014) 256401.
[23] R.W. Zhang, et al., J. Mater. Chem. C 4 (2016) 2088–2094.
[24] Z. Qiao, et al., PRL 112 (2014) 116404-1–116404-5.
[25] M. Karplus, J.A. McCammon, Nat. Struct. Mol. Biol. 9 (9) (2002) 646.
[26] R.W. Zhang, et al., New J. Phys. 17 (2015) 083036-1–083036-8.
[27] Y.P. Wang, et al., Appl. Phys. Lett. 108 (2016) 073104-1–073104-5.
[28] S.S. Li, et al., ACS Appl. Mater. Interfaces 9 (47) (2017) 41443–41453.
[29] S. Plimpton, J. Comp. Phys. 117 (1995) 1–19.
[30] A. Stukowski, Model. Simul. Mater. Sci. Eng. 18 (2010) 015012.
[31] X.W. Zhou, et al., Phys. Rev. B 69 (2004) 144113.
[32] A. Landa, et al., Acta mater. 48 (2000) 1753–1761.
[33] M. Koga, et al., J. Phys. Soc. Jpn. 86 (2017) 054703.
[34] J.H. Han, T. Oda, Phys. Chem. Chem. Phys. 19 (15) (2017) 9945–9956.
[35] D. Mason, J. Phys..: Condens. Matter 27 (2015) 145401.
[36] J. Li, Basic Molecular Dynamics, Handbook of Materials Modeling, Springer Publishing, 2005.
[37] J. Tersoff, Phys. Rev. B 39 (1989) 5566–5568.
[38] D. Datta, B. Pal, B. Chaudhuri, Elements of Physics 1, General properties of matter, Elasticity, Publishing Syndicate Publishing, 2002.